Cryst. Res. Technol.	31	1996	S	135–142

I. AKSENOV*, K. SATO, T. SHINZATO, N. NISHIKAWA and H. NAKANISHI†

Faculty of Technology, Tokyo University of Agriculture and Technology, Koganei, Tokyo 184, Japan
*Optoelectronics Division, Electrotechnical Laboratory,Tsukuba, Ibaraki 305, Japan
†Faculty of Science and Technology, Science University of Tokyo, Noda, Chiba 278, Japan

FREE-CARRIER AND INTRABAND ABSORPTION IN $CuInSe_2$

The infrared (IR) absorption and ESR spectra of the $CuInSe_2$ (CIS) crystals, grown by the normal freezing technique and subsequently annealed in various atmospheres, have been studied in connection with the annealing-induced motion of the Fermi level relative to the energy band edges. The degenerate n-type crystals exhibited a free-electron absorption, while the p-type crystals showed both an intra-valence-band and a free-hole absorption, from the analysis of which the energy positions of the Fermi level have been evaluated, and the electrical parameters of the respective crystals have been estimated.

In the ESR spectra the signals from iron residual impurity in its both divalent and trivalent charged states, as well as the signals arising from native defects V_{Cu} and In_{Cu}, have been detected, the intensities of the ESR signals being dependent on the composition of the samples and the Fermi level position.

1. INTRODUCTION

Ternary chalcopyrite semiconductor $CuInSe_2$ (CIS) is considered to be a promising material for solar cell applications because of its high ($>10^{-4}$ cm^{-1}) optical absorption coefficient, a desirable for photovoltaics direct band gap E_g = 1.08 eV, as well as its versatile optical and electrical properties which can, in principle, be tuned for the specific needs in a particular device structure.

In order to actually realize the said tuning of the characteristics of CIS it is vital to know the dependence of the electro-optical properties of this material on the energy position of the electrochemical potential (Fermi level) in relation to the band edges, since the position of the Fermi level determines the physical properties of semiconductors, i.e. the conductivity type, carrier concentrations, as well as the charged states of deep centres, including those formed by residual transition atom ions (AKSENOV et.al). The position of the Fermi level relative to the band edges can be influenced by thermal treatments of the material due to the annealing-induced changes in the material stoichiometry, as well as changes in the concentrations of intrinsic and extrinsic defects.

In this study we report the results of the infrared (IR) optical absorption and electron spin resonance (ESR) investigations of the CIS single crystals in connection with the annealing-induced motion of the Fermi level relative to the band edges of CIS.

2. EXPERIMENTAL

Single crystals of CIS were grown by the normal freezing method, when the constituent elements (Cu, In, and S of 99.9999% purity) were heated up to 1150°C with subsequent slow cooling with the rate 5°C/hr (ENDO et.al). Thermal annealings of the crystals in vacuum, Se-vapour and in the presence of Cu were carried out for 50 hr at 650°C.

The obtained crystals were characterized by the thermal probe and four-probe methods to determine their resistivities and conductivity type, respectively, as well as by the electron probe microanalysis (EPMA) to determine their composition.

Optical absorption measurements were carried out at room temperature (RT) by using a BOMEM Fourier Transform IR spectrometer, whereas ESR spectra were taken at 4.2 K with a JEOL X-band spectrometer with the microwave power of 5 mW.

3. RESULTS AND DISCUSSION

3.1. Samples characterization

The composition and electrical properties of the $CuInSe_2$ crystals - as-grown and annealed in various atmospheres - are shown in Table 1. It can be seen that the as-grown and Se-vapour annealed samples exhibit highly conductive p-type conductivity, whereas annealing of the as-grown samples in vacuum or in the presence of Cu turns them highly conductive or semi-insulating n-type, respectively. On the basis of EPMA results and taking into account the defect chemistry model of ternary compounds (GROENINK et.al), the deviation of the actual composition of our samples from the ideal formula $CuInSe_2$ has been described by two parameters $\Delta x = [Cu]/[In] - 1$ and $\Delta y = 2[Se]/([Cu] + 3[In]) - 1$ (where [ ] is the total concentration of respective atoms in the sample), which determine the deviation from molecularity and valence stoichiometry, respectively.

Table 1. Annealing-induced changes in the composition and electrical properties of CIS crystals

Samples	as-grown	vacuum	Cu-vapour	Se-vapour
Conductivity type	p	n	n	p
Resistivity (Ohm cm)	10^{-1}	1	10^{3}	10^{-1}
Cu (at %)	26	25	29	23
In (at %)	24	28	26	25
Se (at %)	50	47	45	52
Δx	>0	<0	>0	<0
Δy	~ 0	<0	<0	>0
Majority Defects	V_{In}, Cu_{In}	V_{Cu}, In_{Cu} V_{Se}	V_{In}, Cu_{In} V_{Se}	V_{Cu}, In_{Cu}

Analysis of the parameters Δx and Δy combined with the data on the formation energies of the defects in CIS (NEUMANN) allows us to figure out the most probable native defects in the as-grown and annealed crystals, these majority defects being also shown in Table 1. From these native defects, expected from the defect chemistry considerations, we were able to observe two defects, namely V_{Cu} and In_{Cu}, in the ESR spectra discussed below.

3.2. IR absorption

3.2.1. General observations

The typical IR absorption spectra of the as-grown and annealed CIS crystals are shown in Fig. 1. The as-grown samples exhibit a broad absorption A-band peaked at about 3000 cm^{-1} (0.36 eV), which was found to be quenched by annealing in vacuum or in the presence of Cu. Annealing in Se-vapour, to the contrary, results in an enhancement of the A-band, as well as in an appearance of an absorption B-band at lower energies (1200 cm^{-1} = 0.14 eV).

Since the A- and B-bands were observed only in the highly conductive p-type samples, and by analogy with the results on the IR absorption studies in Ge (KAISER et.al) and GaAs (BRAUNSTEIN et.al), we believe that these bands originate from intraband transitions between subbands of the valence band of CIS, split by spin-orbit interaction.

The sharp rise of absorption at the low-energy side of the spectra, shown in Fig. 1, has been attributed to the free-carrier absorption, which is known to be observable in semiconductors at high enough carrier concentrations (SPITZER et.al). Indeed, we could not observe this absorption in the semi-insulating samples (Cu-annealed) due to the low concentration of the free carriers in those samples.

Therefore, the IR absorption spectra of the p-type CIS crystals, shown in Fig. 2, are thought to be composed of two components, i.e. the component due to the intra-valence-band absorption and that due to the free-hole absorption; whereas the spectrum of the highly conductive n-type sample (vacuum-annealed) is believed to originate from the free-electron absorption in the conduction band.

For the vacuum-annealed samples we have also been able to observe an annealing-induced shift of the fundamental band-to-band absorption from E_g = 0.95 eV to E_g' = 0.96 eV (the spectra are not shown), attributed to an upward shift of the Fermi level, with the resulting Fermi level position being situated above the bottom of the conduction band. Therefore, the electrons in the conduction band of the vacuum-annealed samples are degenerate, which is expected to be easily

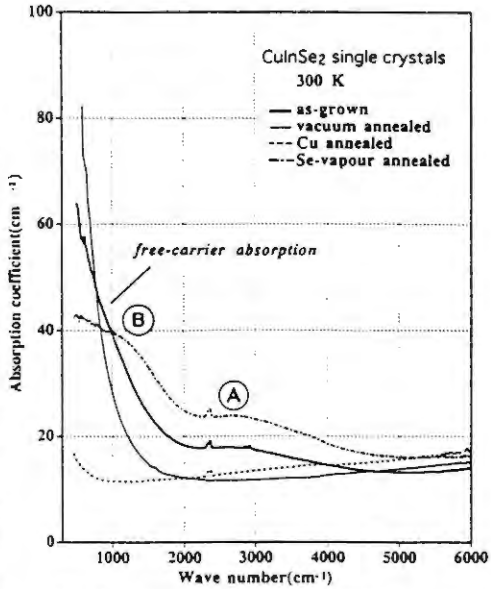

Fig. 1. IR absorption spectra of CIS crystals.

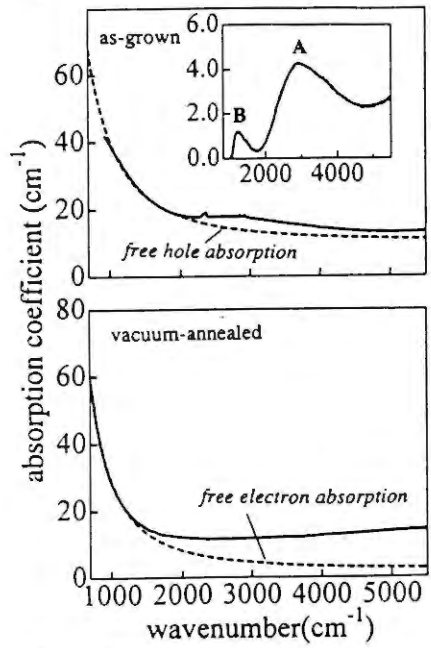

Fig. 2. Spectra of the crystals together with computer fits for the free-carrier absorption. The difference between the measured absorption coefficient and that calculated for the free-hole absorption is shown in the inset - it represents the intraband absorption spectrum.

achieved owing to the low value of the effective mass m_e of the electrons in CIS (m_e = 0.09 m_o, where m_o is the free electron mass (NEUMANN)), implying a sharp curvature of the conduction band and a low density of states near its bottom.

For a degenerate n-type semiconductor the optical band gap E_g' is given by a separation between the lowest unfilled level in the conduction band E_{en} and the corresponding level E_{hn} in the valence band, which lie approximately $4k_BT$ below the Fermi level E_f and $(m_e/m_h)(E_{en} - E_c)$ below the top of the valence band, respectively. The shift of the fundamental absorption edge is given by

$$\Delta E_g = E_g' - E_g = (1 + m_e/m_h)(E_f - E_c - 4k_BT) , \qquad (1)$$

where m_e/m_h takes into account the momentum conservation during optical transition.

Using m_e=0.09 m_o and m_{hh}=0.71 m_o (NEUMANN), from Eq.(1) the Fermi level E_{fn} in the vacuum-annealed sample is found to lie ~109 meV above the bottom of the conduction band at RT. The optical band-to-band transitions then occur between the lowest unfilled level E_{en} in the conduction band positioned ~ 9 meV above the conduction band bottom (Fig. 3) and the corresponding level in the valence band E_{hn}, which satisfies the momentum conservation rule (vertical transition) and lies ~ 1 meV below the top of the valence band.

3.2.2. Intraband absorption

The energy band structure of CIS is shown in Fig. 3, with the information relevant to this section being in the lower part of this figure. By the effect of the non-cubic crystal field (Δ_{cf}) combined with the spin-orbit interaction (Δ_{so}) the Γ_{15} uppermost valence band of the zincblende structure is split into three components having the symmetry Γ_6^5, Γ_7^4 and Γ_7^5, where the upper indices indicate the single-group representation from which the double-group representation, shown by lower indices and taking into account the spin-orbit interaction, originates. The positions of the Γ_7^4 and Γ_7^5 energy levels relative to that of the uppermost Γ_6^5 level are given by (NEUMANN)

$$E(\Gamma_7^{4,5}) - E(\Gamma_6^5) = \Delta_{1,2} = -\frac{1}{2}(\Delta_{cf} + \Delta_{so}) \pm \frac{1}{2}\left[(\Delta_{cf} + \Delta_{so})^2 - \frac{8}{3}\Delta_{cf}\Delta_{so}\right]^{1/2} , \qquad (2)$$

where Δ_{cf} = 0.006 eV and Δ_{so} = 0.233 eV.The values of Δ_1 and Δ_2 , evaluated from Eq.(2) and shown in Fig. 3, are 0.003 eV and 0.236 eV, respectively. The crystal field splitting of the valence band in CIS is very small, which is a result of a small tetragonal distortion of the CIS crystal lattice (c/a = 2.007).

Since the momentum of a photon is negligible compared to the crystal momentum (the momentum of a carrier in an energy band), the momentum of the electron should be conserved in the photo-absorption process. The electron, hence, will experience the vertical transition on the energy level diagram, shown in Fig. 3, with the initial state and the final state having the same momentum k_1. In the parabolic energy bands approximation we can write for the absorption A-band

$$E_{hp} = \hbar^2 k_1^2 / 2m_{hh} , \qquad (3)$$

$$E_A = \Delta_1 + \Delta_2 - E_{hp} + \hbar^2 k_1^2 / 2m_{sh} , \qquad (4)$$

where E_{hp} is the energy of the lowest unfilled level in the valence band for the p-type crystals (the energy of the final state of the electron transition), and m_{hh}, m_{sh} are the effective masses of holes in the respective valence subbands (see Fig. 3).

From Eq.(3) and (4) we can determine the energy position of the level E_{hp} inside the valence band as being E_{hp} = -18 meV. Now, having known the position of the final state of the inter-valence-band transitions and repeating the similar calculations for the transition between Γ_7^4 and Γ_6^5 valence subbands we find out that this transition should take place at the energy of 0.145 eV, which is exactly the spectral position of the peak of the B-band, shown in Figs. 1 and 2.

We, therefore, attribute the experimentally observed A- and B-bands in the IR absorption spectra of the p-type crystals to the transitions from the Γ_7^5 and Γ_7^4 valence subbands to the Γ_6^5 valence subband (see Fig. 3). Since the level E_{hp} lies about $4k_BT$ below the Fermi level for the p-type samples, we can determine the Fermi level position for the p-type samples as being E_{fp} = 82 meV. The Fermi level, therefore, lies inside the band gap, and the p-type crystals are non-degenerate.

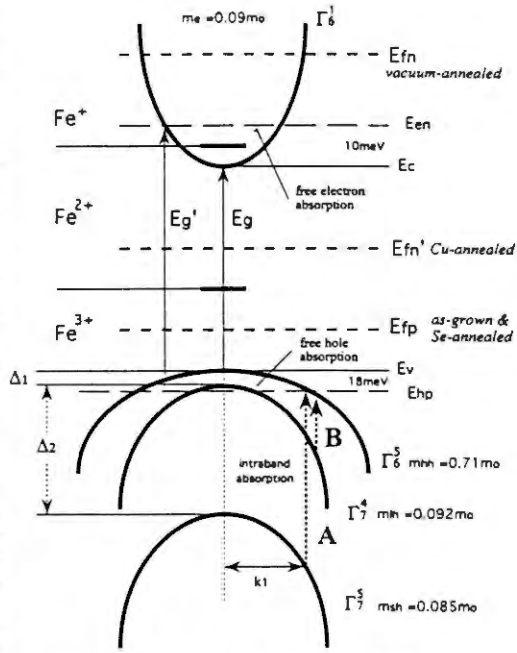

Fig. 3. The energy level diagram, showing the band structure of CIS. See text for details.

3.2.3. Free-carrier absorption

As was discussed in section 3.2.1, from the optical absorption measurements near the band-edge it was found that the Fermi level in our highly conductive degenerate n-type samples lies about 109 meV above the bottom of the conduction band. Knowing the position of the Fermi level in the degenerate parabolic conduction band, as well as the electron effective mass, we can estimate the electron concentration in these samples from the expression (PANKOVE et.al)

$$n_e = 4\pi\left(\frac{2m_e}{h^2}\right)^{3/2}\int_{E_c}^{\infty}\frac{E^{1/2}}{1+\exp\left[\left(E-E_f\right)/k_BT\right]}dE \quad , \tag{5}$$

as being $n_e \approx 7\times10^{18}$ cm^{-3}. For the concentration of holes in the p-type (non-degenerate) samples we can write

$$n_p = 2\left(2\pi m_h k_BT/h^2\right)^{3/2}\exp\left[\left(E_v-E_f\right)/k_BT\right] \quad . \tag{6}$$

where, since the temperature at which our experiment was conducted (k_BT ~ 25 meV) greatly exceeds the value of Δ_1 = 3 meV, we introduced the effective density of states hole mass $m_h = (m_{hh}^{3/2} + m_{lh}^{3/2})^{2/3} = 0.73\ m_o$. From Eq.(6) we obtain the RT concentration of holes in our p-type samples as $n_p \approx 5.6\times10^{17}$ cm^{-3}.

Knowing the concentrations of carriers in the respective energy bands, we can calculate the free-carrier absorption coefficient α_f by using the classical (Drude) formula as

$$\alpha_f = \frac{\omega_p^2 \tau}{n_o c \varepsilon_o} \frac{1}{\omega^j \tau^2 + 1} \quad , \tag{7}$$

where n_o is the index of refraction, τ is the carrier relaxation time, j is the fitting parameter and $\omega_p = (n_i e^2 / m_i \varepsilon_o)^{1/2}$ is the plasma frequency with n_i and m_i (i = e,h) being the concentrations and effective masses of the carriers in respective energy bands. Fig. 2 shows the best fits of α_f, given by Eq.(7), to the experimental IR absorption spectra for the degenerate p-type (as-grown) and n-type (vacuum-annealed) CIS crystals. From these computer fits we deduced the values of the fitting parameter j and the carrier relaxation times for electrons and holes as being $\tau_e \sim 40$ fs and $\tau_p \sim 13$ fs. Then, knowing the relaxation times and using the classical expression $\mu_i = e\tau_i / m_i$, we estimated the electron and hole mobilities in our crystals as $\mu_e \sim 730$ cm^2/Vs and $\mu_h \sim 30$ cm^2/Vs, the estimated values being in the range of those previously reported for CIS (NEUMANN). From the values of the fitting parameter $j \sim 2$ for carriers we conclude that the dominant mechanism of scattering in our samples at RT is the scattering by phonons, in accordance with the results of electrical measurements (WASIM).

3.3. ESR

3.3.1. The assignment of signals

The typical ESR spectra of the as-grown and annealed CIS crystals are shown in Fig. 4(a). The spectrum of the as-grown sample exhibit a complex signal, marked as I-signal and consisting of both isotropic and anisotropic components. The signal is centred on g = 4.3 and is believed to originate from Fe^{3+} in a strong non-cubic ligand field. The Hamiltonian of the Fe^{3+} ion ($^6S_{5/2}$) in the non-cubic crystal field reads (HOLTON et.al)

$$H = g \beta \mathbf{H S} + D[S_z^2 - 1/3S(S+1)] + E(S_x^2 - S_y^2) \quad , \tag{8}$$

where D and E are parameters of the axial and rhombic components of the crystal field, respectively.

Both the axial and rhombic components of the ligand field cause the splitting of the six-fold-degenerate ground state $^6S_{5/2}$ of Fe^{3+} into three Kramers doublets, resulting in the possibility of observation of the ESR signal. The solutions of the above Hamiltonian depend on the parameter $\lambda = E/D$, describing the relative strength of the axial and rhombic terms of the crystal field. If $E \gg D$, we should observe a nearly isotropic signal near g = 4.3, which is in accordance with our results and has also been observed for Fe^{3+}-X pairs in $AgGaS_2$ (BARDELEBEN et.al). For the second limiting case, when $E \ll D$, we may expect an anisotropic signal consisting of several lines with g-values in the range 2 – 6, which has also been detected in our CIS crystals.

We believe, therefore, that the Fe^{3+} ion in our samples form two different complex defects of the type Fe^{3+}-X, one of which results in the strong axial field and the other - in the strong rhombic field of ligands on the site of Fe^{3+} in the crystal lattice. Further studies are needed to figure out the nature of the X-centres.

It can be seen from Fig. 4 that annealing of the crystals in vacuum results in a quenching of the Fe^{3+}-originated signal and in an appearance of four new signals: a highly anisotropic signal marked as II, as well as three isotropic signals marked as III, IV and

V, which are shown in detail in Fig. 4 (b). The annealing in the presence of Cu partly quenches the Fe^{3+}-related signal and also leads to an appearance of the II-signal, whereas annealing in Se-vapour results in quenching of the II-signal and an appearance of the III-signal.

The highly anisotropic II-signal with the peak-to-peak line width ΔH_{pp} = 4 mT, the effective g-factor of which takes its maximum value of $g_{eff//}$ = 28.7 when the tetragonal c-axis of the crystal is parallel to the external magnetic field, has been observed in $CuAlS_2$ (KAUFMANN) and CIS (TCHAPKUI-NIAT et.al), and has been attributed to the substitutional divalent iron impurity, the signal originating from the magnetically allowed microwave transitions 2 ⇔ -2 within the lowest M_S=± 2 non-Kramers doublet.

The isotropic III-signal with g = 2.12 and ΔH_{pp} = 10 mT has been attributed to the signal from hole trapped by copper vacancy, the signal being broadened by the hyperfine interaction with In nuclei (bearing the nuclear spin I = 9/2) in the second shell surrounding of the V_{Cu}-defect. The assignment of this signal has been made on the basis of the reported results (TCHAPKUI-NIAT et.al; PADAM et.al), the assignment being in agreement with the fact that this signal was observed only in Cu-deficient samples (vacuum- or Se-annealed) with $\Delta x < 0$ (see Table 1).

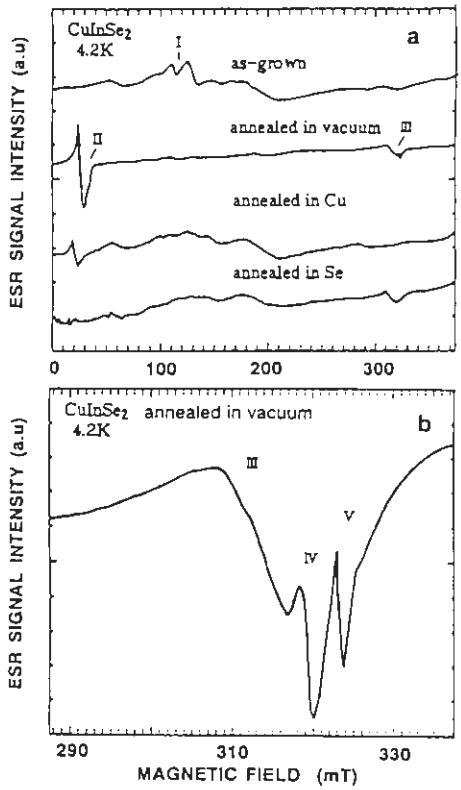

Fig. 4. ESR spectra of the as-grown and annealed CIS crystals (a) together with detailed spectra of the vacuum-annealed samples (b).

Since the IV- and V-signals, shown in Fig. 4(b) and exhibiting isotropic g-factors of g_{IV} = 2.023 and g_V = 2.002, were observed only in the highly conductive n-type samples, they are believed to originate from electrons. The IV-signal may originate from electrons in a selenium-depleted phase $CuIn_2Se_{3.5}$ (TCHAPKUI-NIAT et.al), while the V-signal has been assigned to electrons trapped (at low temperatures of our ESR experiment) by In_{Cu}-donors. The last assignment is in agreement with the previously reported results (PADAM et.al), as well as with the defect chemistry considerations, since for the vacuum annealed samples we can expect the high concentration of the In_{Cu}-defects (Table 1). The narrowness of the IV- and V-signals ($\Delta H_{pp} \approx 0.5$ mT) requires the exchange interaction effects and, therefore, the high concentration of donors, which is also in agreement with the IR absorption results showing that our vacuum-annealed samples are degenerate.

3.3.2. The effect of the Fermi level motion

The observed changes in the ESR spectra of the CIS crystals, caused by thermal treatments in various atmospheres, can be explained by the annealing-induced motion of the Fermi level relative to the energy bands edges.

It was found out from the IR absorption measurements that in the as-grown crystals the Fermi level is situated only about 80 meV above the top of the valence band and, hence,

most probably below the Fe^{2+}/Fe^{3+} demarcation level (Fig. 3, E_{fp}). We, therefore, observe the I-signal from Fe^{3+} in the ESR spectra of the as-grown samples.

Annealing in vacuum or Cu-atmosphere leads to the change of the conductivity type, the samples being converted, respectively, into the degenerate or semi-insulating n-type ones. These results indicate that the Fermi level is shifted upwards and is positioned inside the conduction band (vacuum-annealed samples, Fig. 3, E_{fn}) or in the band gap above the Fe^{2+}/Fe^{3+} demarcation level (Cu-annealed samples, Fig. 3, E_{fn}'). We, therefore, observe the quenching of the Fe^{3+}-originated signal and an appearance of the II-signal from Fe^{2+}. Annealing in vacuum also results in a drastic increase in the concentration of the V_{Cu}- and In_{Cu}-defects (Table 1), which leads to an appearance of the signals from carriers trapped by these defects.

The annealing in the Se-vapour results in a reverse process, the Fermi level being shifted down to the valence band (and below the Fe^{2+}/Fe^{3+} demarcation level), which results in the highly conductive p-type conductivity and in the quenching of the ESR signal from Fe^{2+}.

It should be pointed out that the Fe^{2+}-originated II-signal was found to be quenched down to about one-half of its original intensity by an illumination with infrared light (a 1.06 μm line of YAG laser was used as an excitation source) in the semi-insulating n-type samples (Cu-annealed), but exhibits no changes under the same illumination in the degenerate n-type samples (vacuum-annealed). This phenomena can be explained assuming that the Fe^{+}/Fe^{2+} demarcation level is in resonance with the conduction band of CIS, i.e. lies inside of the conduction band (Fig. 3). Then, in the semi-insulating crystals, under IR light excitation some of the Fe^{2+} ions capture electrons from the valence band and become monovalent, i.e. $Fe^{2+} + e^{-} \Rightarrow Fe^{+}$, which results in the quenching of the Fe^{2+}- originated ESR signal. The last photo-ionization process, however, becomes impossible in degenerate samples if the Fe^{+}/Fe^{2+} demarcation level is situated below the level E_{en} (Fig. 3) in the conduction band, since electronic transitions to the completely filled states are impossible. We, therefore, believe that while the Fe^{2+}/Fe^{3+} demarcation level is situated in the band gap of CIS, the Fe^{+}/Fe^{2+} demarcation level is in resonance with the conduction band.

References

AKSENOV, I., SATO, K.: Jpn. J. Appl. Phys. **31** (1992) 2352
BARDELEBEN, H.J., GOLTZENE, A., SCHWAB, C., FEIGELSON, R.S.: Phys. Rev. B **5** (1980) 1757
BRAUNSTEIN, R., KANE, E.O.: J. Phys. Chem. Solids **23** (1962) 1423
ENDO, S., IRIE, T., NAKANISHI, H.: Solar Cells **16** (1986) 1
GROENINK, J.A., JANSE, P.H.: Z. Phys. Chem., **110** (1978) 17
HOLTON, W.C., DE WIT, M., ESTLE, T.M., DISCHER, B., SCHNEIDER, D.: Phys. Rev. **169** (1968) 359
KAISER, W., COLLINS, R.J., FAN, H.Y.: Phys. Rev. **91** (1953) 1380
KAUFMANN, U.: Solid State Commun. **19** (1976) 213
NEUMANN, H.: Solar Cells **16** (1986) 317
PADAM, G.K., MALHOTTA, G.L., GUPTA, S.K.: Solar Energy Mater. **22** (1991) 303
PANKOVE, J.I., ANNAVEDDER, E.K.: J. Appl. Phys. **36** (1965) 3948
SPITZER, W.G., WHELAN, J.M.: Phys. Rev. **114** (1959) 59
TCHAPKUI-NIAT, J.M., GOLTZENE, A., SCHWAB, C.: J. Phys. C: Solid State Phys. **15** (1982) 4671
WASIM, S.M.: Solar Cells **16** (1986) 289